Monte Carlo study of the beam shaping assembly optimization for providing high epithermal neutron flux for BNCT based on D–T neutron generator

Shuang Hang, Xiaobin Tang, Diyun Shu, Yuanhao Liu, Changran Geng, Chunhui Gong, Haiyan Yu & Da Chen

Journal of Radioanalytical and Nuclear Chemistry
An International Journal Dealing with All Aspects and Applications of Nuclear Chemistry

ISSN 0236-5731
Volume 310
Number 3

J Radioanal Nucl Chem (2016)
310:1289-1298
DOI 10.1007/s10967-016-5001-4

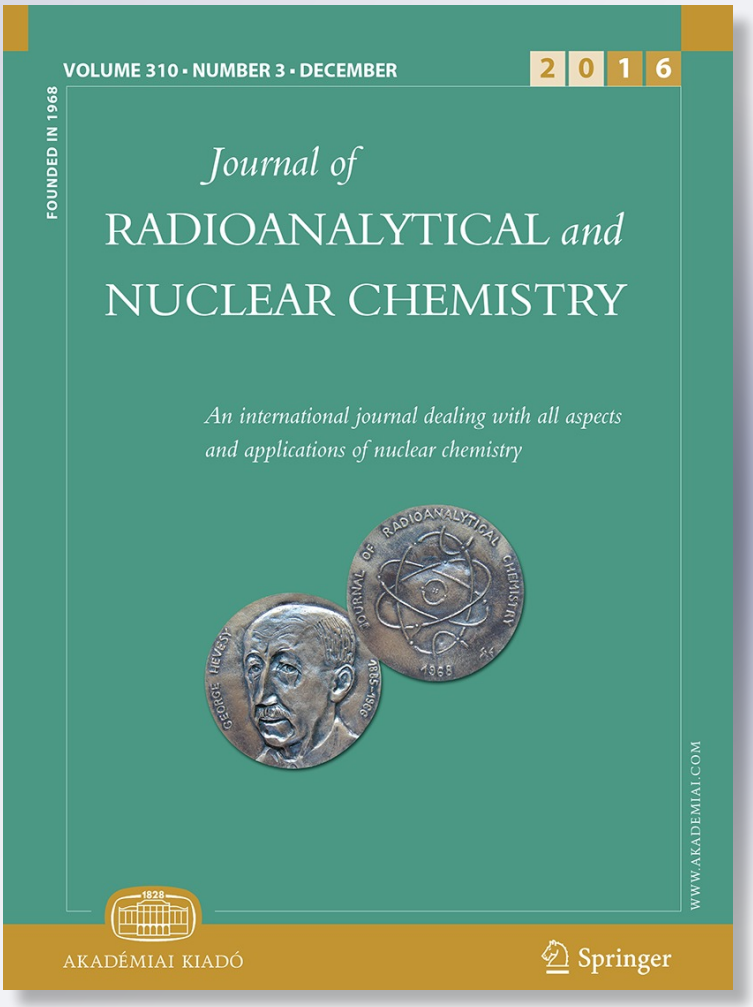

Springer

J Radioanal Nucl Chem (2016) 310:1289–1298
DOI 10.1007/s10967-016-5001-4

Monte Carlo study of the beam shaping assembly optimization for providing high epithermal neutron flux for BNCT based on D–T neutron generator

Shuang Hang[1] · Xiaobin Tang[1,2] · Diyun Shu[1] · Yuanhao Liu[1] · Changran Geng[1,3] · Chunhui Gong[1] · Haiyan Yu[1] · Da Chen[1,2]

Received: 25 April 2016 / Published online: 29 August 2016

Abstract In this study, a beam shaping assembly with high epithermal neutron flux output was designed based on a D–T neutron generator using Monte Carlo N-particle Transport Code. D_2O-^{54}Fe and AlF_3-^{60}Ni interlayer moderator, efficient multiplier, filters, and reflector were used to improve the neutron beam quality according to the requirements of boron neutron capture therapy while maintaining high flux of epithermal neutron beam. In addition, the dose performance of the beam from our proposed facility was assessed in the Snyder head phantom. The simulation results proved that the proposed neutron beam was applicable to the treatment of deep-seated brain tumor.

Keywords Boron neutron capture therapy · D-T neutron generator · Beam shaping assembly · Deep-seated brain tumor · Dosimetric assessment · MCNP

✉ Xiaobin Tang
tangxiaobin@nuaa.edu.cn

[1] Department of Nuclear Science & Engineering, Nanjing University of Aeronautics and Astronautics, 29 Yudao St., Nanjing 210016, China

[2] Collaborative Innovation Center of Radiation Medicine of Jiangsu Higher Education Institutions, 29 Yudao St., Nanjing 210016, China

[3] Department of Radiation Oncology, Massachusetts General Hospital, Boston, MA 02114, USA

Introduction

With the precise and selective role of targeting tumor cells, boron neutron capture therapy (BNCT) is a promising oncotherapy approach. BNCT treats the tumor by two heavy fragments (^7Li and α-particle) with high linear energy transfer (LET) and relative biological effectiveness (RBE), generated in the process of capture reaction between boron and the low-energy neutrons [1–4]. In order to treat the deep-seated tumors, epithermal neutrons with an energy range between 1 and 10 keV is indispensable. However, the development of high performance epithermal neutron beam is one of the crucial technical bottlenecks of BNCT.

As the energy of the neutron beams from available neutron sources is too high, beam shaping assemblies (BSA) should make the neutron beams suitable for BNCT treatment. The optimization design of BSA is the critical step to improve the performance of neutron beam and the treatment effect of BNCT. Many optimum neutron BSAs have been developed for different neutron sources, especially in the recent decades. The reactor is used as the earliest BNCT neutron source. BSAs based on fission reactors have been constructed at numerous reactors worldwide to generate epithermal neutron beams [5–7]. The accelerator driven neutron sources which can be constructed easily in the hospital have also been developed for clinical use. The neutron beam generated by the accelerator should be optimized more carefully since the neutron yield is not so high and high energy component is larger than that of the reactor. More detailed optimization of BSAs based on the accelerators has been investigated [8–10].

In previous studies, the BNCT facilities designs showed the compact and convenient tendency. According to the development tendency, the D-T neutron generator is a

suitable neutron source for BNCT because of the following advantages [11–14]. First, it has the high neutron yield, approximate monoenergetic neutron output and low γ photon emission. Second, it does not require high-energy accelerator. Third, it is characterized by the compact structure, low price, good security, and convenient deployment in the hospital. As the energy of the neutron from the D-T neutron generator is 14.1 MeV, a BSA is required to obtain the neutron beam output according to the requirements of BNCT.

The BSA based on the D-T neutron generator generally includes several parts: neutron multiplier, moderator, filters, reflector and collimator. The neutron multiplier is adjacent to the neutron source to increase neutron flux based on (*n*, *2n*) and (*n*, *3n*) reactions in the fast neutron region. The moderator is used to moderate the fast neutrons output from the neutron multiplier into the epithermal neutrons. The filters are required to reduce the damage to patients' healthy tissue caused by the impurities in the epithermal neutron beam such as fast neutrons, thermal neutrons and gamma rays. The reflector should guide the epithermal neutrons to the beam port and prevent the neutrons in the desired energy escaping from the configuration. The collimator is used to decrease the beam port size to a flat circular surface with a diameter of 12 cm to avoid excessive dose to adjacent healthy tissues.

In the study of BSA, two criteria should be considered. In the BSA optimization, the output of the neutron beam should meet the "BNCT in-air beam port recommended quality parameters" (Table 1), which is combined with the IAEA recommended limits and some other parameters commonly used in BSA optimization. In order to minimize the treatment time in BNCT, the epithermal neutron flux has to be high enough ($>10^9$ n cm^{-2} s^{-1}); $\phi_{epithermal}/\phi_{fast}$, $\phi_{epithermal}/\phi_{thermal}$, $\dot{D}_{fast}/\phi_{epithermal}$, and $\dot{D}_{\gamma}/\phi_{epithermal}$ are the criteria of impurities in the neutron beam. The lower contents of fast neutron, thermal neutron, γ-photon component are helpful to reduce the damage to healthy tissue in patients. J/ϕ is the angular fluence rate weighted cosine of the emergent neutrons at a half space, which provides a measure of the fraction of neutrons that are moving in the forward beam direction. J is the total neutron current, and ϕ is the total neutron flux. The "in-phantom parameters" be taken into account in the dosimetric assessment. Advantage depth dose rate (ADDR) is the maximum delivered dose rate to normal tissue. Considering that the maximum allowable dose to the healthy tissue is 12.5 Gy, the treatment time (TT) can be estimated. Advantage depth (AD) is the depth where the dose to the tumor equals the maximum dose to the normal tissue. It indicates the depth at which the "therapeutic gain" of the beam falls to zero. Therapeutic depth (TD) defines the depth where the tumor dose falls below twice of the maximum dose to normal tissue. Advantage ratio (AR) is the advantage ratio to measure the beam's ability to minimize integral dose to normal tissue while treating the tumor effectively. It is equal to the integral of the total tumor dose divided by the integral of the health tissues dose from 0.0 cm to the AD [15]. The 30 RBE-Gy tumor depth is defined as the depth where the tumor dose falls below 30 RBE-Gy after the treatment.

Table 1 The BNCT in-air beam port recommended quality parameters [23, 27]

BNCT beam port parameters	Limits
$\phi_{epithermal}$	$>10^9$ (n cm^{-2} s^{-1})
$\phi_{epithermal}/\phi_{fast}$	>20
$\phi_{epithermal}/\phi_{thermal}$	>100
$\dot{D}_{fast}/\phi_{epithermal}$	$<2 \times 10^{-13}$ (Gy cm^2)
$\dot{D}_{\gamma}/\phi_{epithermal}$	$<2 \times 10^{-13}$ (Gy cm^2)
J/ϕ	~0.7
Fast energy group	$E > 10$ keV
Epithermal energy group	1 eV $< E <$ 10 keV
Thermal energy group	$E < 1$ eV

Materials and methods

In this study, the MCNP5 code was performed in BSA optimization and dosimetric assessment. All results of simulations are reported with relative error less than 1 %. In MCNP input files, cross section data also include the $S(\alpha, \beta)$ thermal neutron scattering treatment for hydrogen in the body tissue, hydrogen in Polyethylene, and deuterium in heavy water. In BSA optimization, each component of the BSA should be optimized according to the neutron output from the upstream component. When the optimization of each component was finished step by step, the whole BSA model would be established completely. Different parameters needed to be considered according to the purpose of each component.

Neutron source

D-T neutron generator is based on nuclear reaction $T(d, n)^4$He: $T + d = {}^4\text{He} + n + 17.586$ MeV. With the relatively low incident particle energy (120 keV) [16, 17], high neutron yields ($\geq 10^{14}$ n s^{-1}) and approximate monoenergetic neutron output (about 14.1 MeV), D-T neutron generator is a suitable neutron source for BNCT. However, the high energy of the neutrons from the D-T neutron generator is the important challenge in BSA design. Moderation of fast neutrons to epithermal neutrons needs thick moderator

as well as it is difficult to maintain sufficient epithermal neutron flux without fast neutron.

Our research was not based on a particular model of D-T neutron generator and the deuteron straggling in the target was not considered. The initial neutron source was approximately simulated as follows. The neutrons were emitted isotropically across a flat circular surface with the radius of 1.7 cm. The Gaussian fusion energy spectrum defined by the built-in function of MCNP code was employed to describe the energy distribution. The average energy, FWHM, and neutron yield were 14.076, 0.596 MeV, and 1×10^{14} n s^{-1}, respectively. [18, 19]. Compared with previous studies [13, 14], it was an adequate approximation for the BSA optimization.

Neutron multiplier

In the multiplication process, one major concern was whether the material could increase the number of neutrons in the fast region via fission reaction; another one was whether it could reduce the average neutron energy, and make the fast neutron component easy to be moderated. Four materials with relatively high (n, $2n$) reactions cross section at 14.1 MeV was selected as multiplier, i.e. lead, bismuth, natural uranium, and typical commercial enriched uranium (3 %) [12, 20, 21]. We examined the neutron multiplier materials with different thicknesses and determined the number of neutron per neutron source (N/N_0).

Moderator

The moderator was divided into two parts, i.e. moderator-1 and moderator-2. The main role of the moderator-1 was to moderate the fast neutrons into the epithermal neutrons as more as possible. Therefore, in this layer, the primary concern was epithermal neutron flux $\phi_{epithermal}$ and the secondary concern was $\phi_{epithermal}/\phi_{fast}$ value. Twelve materials was selected as the candidate materials of moderator-1, i.e. MgF_2, D_2O, C_2F_4, Fe, AlF_3, TiF_3, PbF_2, PbF_4, BiF_3, BiF_5, Fluental [22], and Fluental without LiF [18, 23]. The main role of the moderator-2 was to reduce neutron flux while maintaining high epithermal neutron flux. In this layer, the primary concern was $\phi_{epithermal}/\phi_{fast}$ value ($\phi_{epithermal}/\phi_{fast}$ >20) and $\dot{D}_{fast}/\phi_{epithermal}$ value ($<2 \times 10^{-13}$ Gy cm^2) and the secondary concern was $\phi_{epithermal}$ value ($>10^9$ n cm^{-2} s^{-1}). Eight materials was selected as the candidate materials of moderator-2, i.e. MgF_2, AlF_3, Al_2O_3, TiF_3, PbF_4, BiF_5, Fluental, and Fluental without LiF. The candidate materials of the moderator should have the low scattering cross section at the epithermal neutron region, the high scattering cross section at the fast neutron region, and the relatively low neutron absorption cross section. The candidate materials of moderator-1 was more than that of moderator-2, because the candidate materials of moderator-2 not only needs the performance of high epithermal neutron flux output, but also needs the performance of high $\phi_{epithermal}/\phi_{fast}$ value. By simulation, the optimal combinations of the material and thickness of the moderators were obtained. The cylindrical moderators were employed for optimizing the thicknesses of the moderators. As the neutron beam output from the BSA should be focused to the diameter of 12 cm, the radius of the moderator should gradually reduce in the direction of the neutron beam transport.

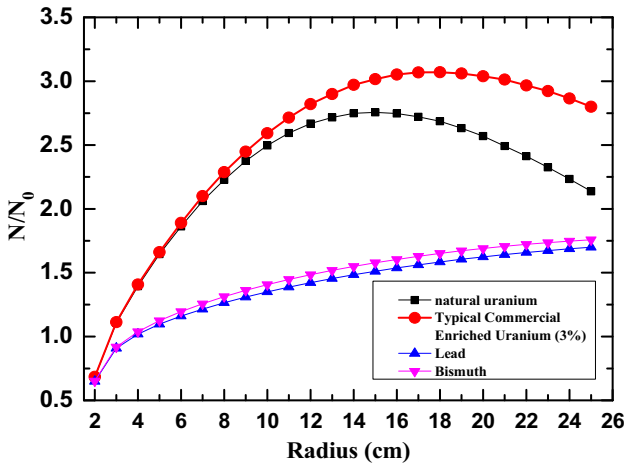

Fig. 1 Number of neutrons in various neutron sources with different thicknesses

Thermal neutron and γ filters

The cylindrical filters were used to optimize the thicknesses of the filters. Li and Cd were chosen as the candidate thermal neutron filter materials. $\phi_{epithermal}/\phi_{thermal}$ (>100) value should be considered during thermal neutron filter optimization. We proposed bismuth as γ filter to reduce gamma rays. In this layer, $\dot{D}_{\gamma}/\phi_{epithermal}$ value ($<2 \times 10^{-13}$ Gy cm^2) should be taken into account.

Dosimetric assessment

In order to estimate the beam performance in tissue, the dose in Snyder head phantom of our proposed neutron beam should be assessed through simulation. The Snyder head phantom was established in MCNP consisted of skin, skull, and brain [24]. The elemental compositions for these structures were from ICRU report 46 [25]. Boron concentration in healthy tissue was set to be 13 ppm and the tumor-skin-normal tissue uptake ratio was 3.6:1.5:1 [19]. The BNCT dose of the neutron beam consists of fast neutron dose, thermal neutron dose, boron dose, and

Table 2 Multiplication efficiency of the candidate materials with their optimized sizes

Multiplier material	Optimization radius (cm)	Multiplication efficiency
3 % enriched uranium	17	3.05
Natural uranium	15	2.76
Lead	25	1.76
Bismuth	25	1.70

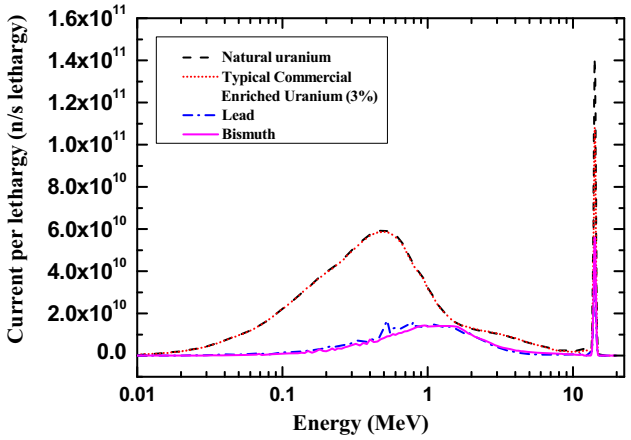

Fig. 2 Neutron current versus the energy on the surface of the neutron multiplier

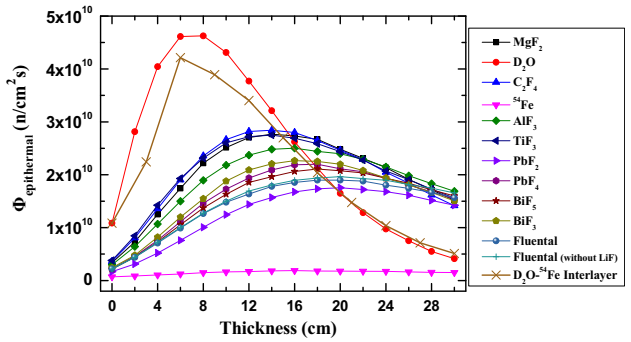

Fig. 3 $\phi_{\text{epithermal}}$ versus the thickness of different moderator-1 materials

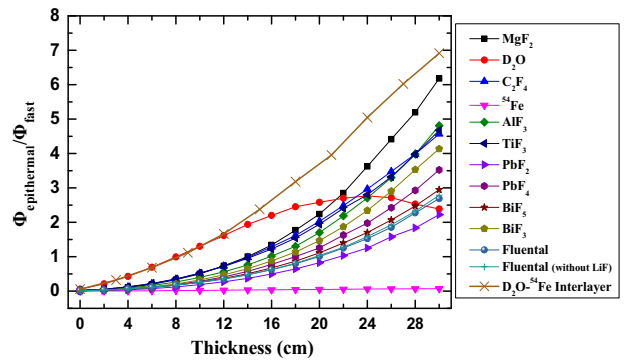

Fig. 4 $\phi_{\text{epithermal}}/\phi_{\text{fast}}$ ratio versus the thickness of different moderator-1 materials

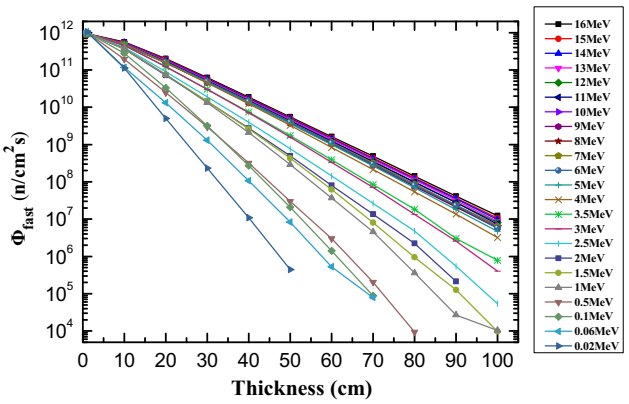

Fig. 5 ϕ_{fast} versus the thickness of MgF_2 of different monoenergetic neutron beams

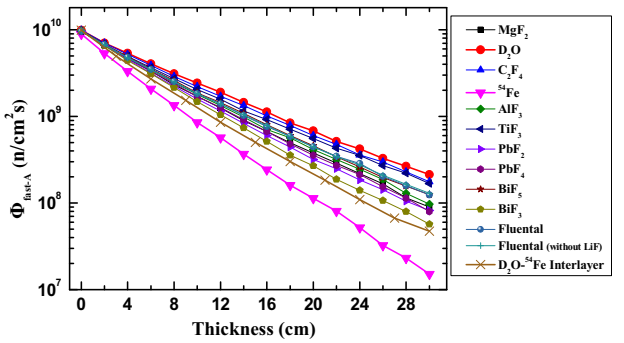

Fig. 6 $\phi_{\text{fast-A}}$ versus the thickness of different moderator-1 materials

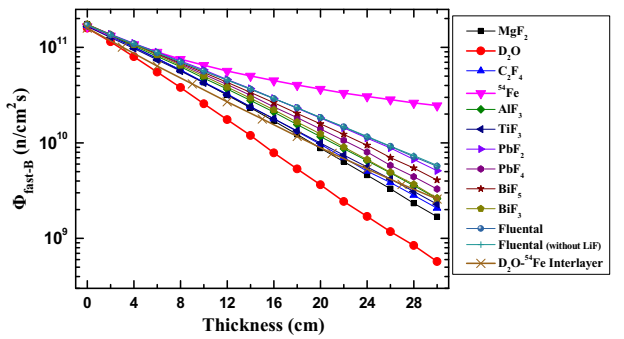

Fig. 7 $\phi_{\text{fast-B}}$ versus the thickness of different moderator-1 materials

gamma dose. Biologically weighted dose is the sum of these physical dose components multiplied by appropriate weights:

Table 3 The neutron beam output from different interlayer materials as moderator-1

Thickness ratio of D_2O-^{54}Fe	Optimization thickness (cm)	$\phi_{epithermal}$ ($\times 10^{10}$ n cm^{-2} s^{-1})	$\phi_{fast\text{-}A}$ ($\times 10^{9}$ n cm^{-2} s^{-1})	$\phi_{fast\text{-}B}$ ($\times 10^{10}$ n cm^{-2} s^{-1})
1:1	6	3.37	2.67	5.67
2:1	6	4.21	2.71	6.39
3:1	8	3.88	2.32	3.64

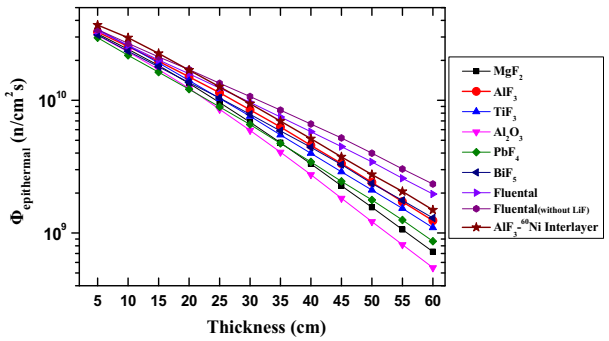

Fig. 8 $\phi_{epithermal}$ versus the thickness of different moderator-2 materials

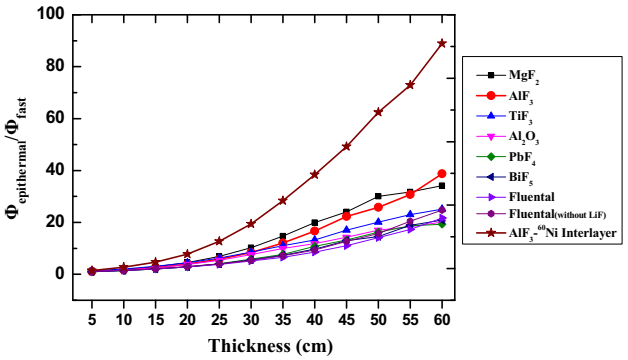

Fig. 9 $\phi_{epithermal}/\phi_{fast}$ ratio versus the thickness of different moderator-2 materials

$$D_{total} = W_N \times D_N + W_{fast} \times D_{fast} + W_B \times D_B + W_\gamma \times D_\gamma \quad (1)$$

where W_N and W_{fast} are 3.2, W_γ is 1, W_B is 3.8 for boron dose in the tumor, 1.3 for boron dose in brain tissue, and 2.5 for boron dose in skin tissue [19].

Results and discussion

Neutron multiplier

In the simulations of various geometric shapes of neutron multipliers, it was found that the spherical neutron multiplier allowed the higher multiplication efficiency [13]. For spherical neutron multiplier, four candidate materials was tested. The number of neutrons per neutron source on the surface of the sphere versus different sphere radius was calculated by F1 tally card (Fig. 1). Obviously, the number of produced neutrons from natural uranium and 3 % in enrichment as a neutron multiplier are the highest. We chose the optimized sizes of four candidate materials and obtained their multiplication efficiency (Table 2). The neutron current versus energy on the neutron multiplier surface of the four candidate materials was calculated. As shown in Fig. 2, neutron multiplier can shift the neutron energy from about 14.1 to 0.1–2 MeV. With the higher neutron number output and less high-energy ($\sim$14 MeV) fast neutron component, spherical 3 % enriched uranium with the radius of 17 cm was chosen as the neutron multiplier.

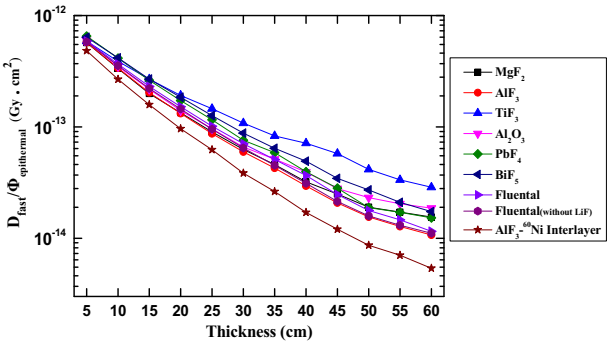

Fig. 10 $\dot{D}_{fast}/\phi_{epithermal}$ ratio versus the thickness of different moderator-2 materials

Moderator

Firstly, the optimal design of the moderator-1 was investigated. The epithermal flux and $\phi_{epithermal}/\phi_{fast}$ of the candidate materials was calculated by MCNP code (Figs. 3, 4). The D_2O allows the higher $\phi_{epithermal}$ of 4.62×10^{10} n cm^{-2} s^{-1} for the moderator with small thickness (7 cm), although the flux level quickly drops with the increase in the thickness. For D_2O, the maximum value of $\phi_{epithermal}/\phi_{fast}$ is about 2.5. The 12 cm thick MgF_2 provides a good balance between $\phi_{epithermal}$ and $\phi_{epithermal}/\phi_{fast}$ ratios, but the maximum $\phi_{epithermal}$ value of MgF_2 is about 60 % of the value of D_2O. After extensive simulation, it is found that, if 7 cm D_2O was chosen as

Table 4 The neutron beam output from different interlayer materials as moderator-2

Thickness ratio of AlF_3-^{60}Ni	Optimization thickness (cm)	$\phi_{epithermal}$ ($\times 10^9$ n cm^{-2} s^{-1})	$\phi_{epithermal}/\phi_{fast}$
3:1	40	5.34	42.23
4:1	40	6.96	38.41
5:1	36	6.40	29.01

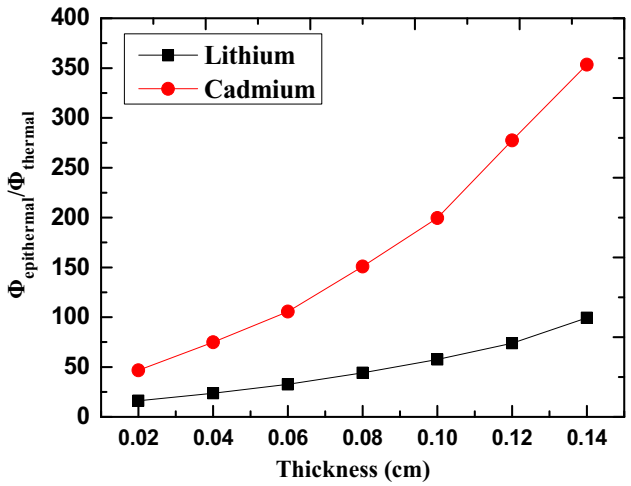

Fig. 11 $\phi_{epithermal}/\phi_{thermal}$ ratio versus the thickness of the thermal neutron filter

moderator-1, even though the material which could quickly increase $\phi_{epithermal}/\phi_{fast}$ value was chosen as moderator-2, it was still difficult to make $\phi_{epithermal}$ and $\phi_{epithermal}/\phi_{fast}$ to meet the in-air parameters simultaneously. In the following study, we are going to explore potential reasons.

In order to discover the reason that the fast neutrons output from the moderator-1 made of D_2O is difficult to be removed. It is necessary to explore the performance of the candidate materials to moderate the monoenergetic fast neutron beams with different energies. In this simulation, neutron source was set as the monoenergetic fast neutron

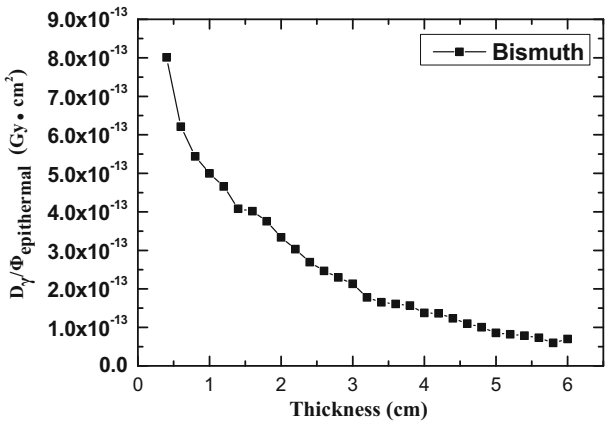

Fig. 12 $\dot{D}_\gamma/\phi_{epithermal}$ ratio versus the thickness of bismuth

beam with different energy levels to represent the fast neutrons output from the moderator-1 made of D_2O, and MgF_2 was chosen as the moderator-2. Then the neutron flux at the exit surface of the moderator was calculated. Figure 5 shows the ϕ_{fast} for MgF_2 as a function of the moderator thickness. According to the experience from previous simulation of moderator-2 optimization, $\phi_{epithermal}$ would reduce to less than 1×10^9 n cm^{-2} s^{-1} when the thickness of MgF_2 was about 60 cm. In this situation, if the ϕ_{fast} was still higher than 1×10^9 n cm^{-2} s^{-1}, even if the fast neutron filter was employed after moderation, we could not make $\phi_{epithermal}/\phi_{fast}$ to reach 20. In Fig. 5, when the thickness of MgF_2 is 60 cm, the flux of the fast neutrons with the initial energy higher than 3 MeV remained relatively high ($\sim 10^9$ n cm^{-2} s^{-1}). Therefore, 3 MeV was chosen as the cut-off point, and we suggested that it was difficult to remove the neutron component from 3 to 16 MeV. The neutron region with the energy level above 3 MeV was classified as Region A, and the neutron region with the energy level between 0.01 and 3 MeV was classified as Region B.

Based on the division of the energy range, Figs. 6 and 7 show the flux of the two neutron regions for the studied materials as a function of the moderator thickness. As shown in Figs. 6 and 7, D_2O has the strongest ability to remove the fast neutrons in the Region B and the weakest ability to remove the fast neutrons in the Region A. The initial flux in Region B was higher than that in Region A, and the fast neutrons in Region B were converted to epithermal neutrons by D_2O. Therefore, D_2O as the moderator-1 could obtain the high epithermal neutron flux, but the large number of fast neutrons in Region A were remained. Fast neutrons in Region A were difficult to be removed. As a result, it was difficult to make $\phi_{epithermal}$ and $\phi_{epithermal}/\phi_{fast}$ to meet the in-air parameters simultaneously. As shown in Figs. 6 and 7, ^{54}Fe has the strongest ability to remove the fast neutrons in the Region A and the weakest ability to remove the fast

Table 5 Comparison between the proposed facility and parallel reflector design

Configurations	$\phi_{epithermal}$ (10^9 n cm^{-2} s^{-1})	$\phi_{epithermal}/\phi_{fast}$
Limits	>1	>20
Arched reflector	4.18	25.72
Vertical reflector	3.74	22.50

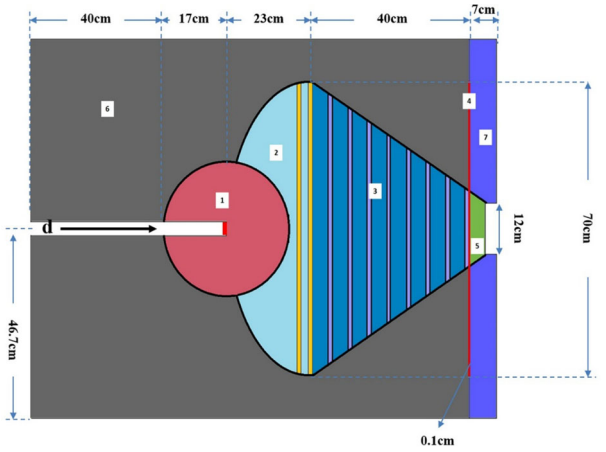

Fig. 13 Cross sectional view of our proposed BSA; *1* Typical commercial enriched uranium as neutron multiplier with the radius of 17 cm, *2* 17 cm D_2O and 6 cm D_2O-^{54}Fe interlayer as the first layer moderator, *3* 40 cm AlF_3-^{60}Ni interlayer as the second layer moderator, *4* 1 mm Cd as the thermal neutron filter, *5* 4 cm Bi as γ filter, *6* Pb as reflector and collimator, *7* 7 cm Li polyethylene as shield

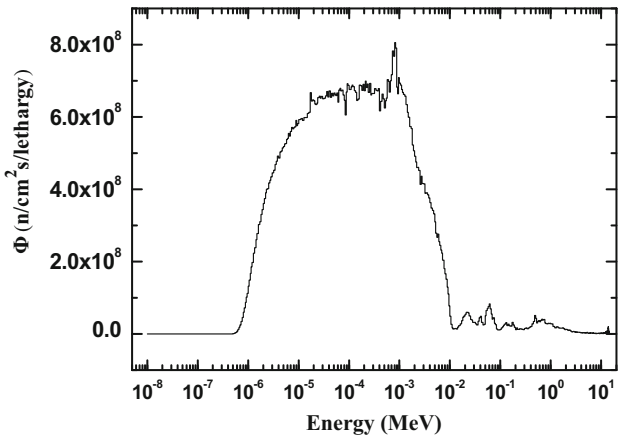

Fig. 14 Neutron beam port spectra of the final BSA configuration

neutrons in the Region B. After extensive computational studies, different thickness ratios of D_2O-^{54}Fe interlayer materials was investigated (Table 3), it is found that the D_2O-^{54}Fe interlayer material with the thickness ratio of 2:1 had the best performance for the two regions (Figs. 6, 7). The thickness ratio 2:1 of D_2O -^{54}Fe interlayer materials means each layer is composed of 2 cm D_2O and 1 cm ^{54}Fe. In Fig. 3, for the D_2O-^{54}Fe interlayer material, the maximum $\phi_{epithermal}$ is 4.21×10^{10} n cm^{-2} s^{-1}, which is 91.13 % of the highest value of D_2O. The performance of $\phi_{epithermal}/\phi_{fast}$ value is much better than that of other candidate materials. Therefore, 6 cm D_2O-^{54}Fe interlayer material with the thickness ratio of 2:1 was chosen as the moderator-1.

For the moderator-2, there is eight candidate materials. The $\phi_{epithermal}$, $\phi_{epithermal}/\phi_{fast}$, and $\dot{D}_{fast}/\phi_{epithermal}$ of the candidate materials versus their thickness are plotted in Figs. 8, 9 and 10 respectively. AlF_3 provided a good balance between increasing $\phi_{epithermal}/\phi_{fast}$ value and maintaining $\phi_{epithermal}$. The combination of AlF_3 and the fast neutron filter material ^{60}Ni to form the interlayer materials was also tested as the moderator-2. We examined different thickness ratios of ^{60}Ni-AlF_3 interlayer materials and found that the thickness ratio of 4:1 was appropriate (Table 4). In Table 4, the thickness ratio of 4:1 provides the highest $\phi_{epithermal}$ value. The $\phi_{epithermal}$ value provided by thickness ratio of 3:1 is only 76.72 % of 4:1 does, although it provides the highest $\phi_{epithermal}/\phi_{fast}$ ratio. Therefore, the thickness ratio of 4:1 made a good balance between $\phi_{epithermal}$ and $\phi_{epithermal}/\phi_{fast}$. Several trends are obvious in Figs. 8, 9 and 10. As expected, performance of AlF_3-^{60}Ni interlayer material with the thickness ratio of 4:1 is much better than that of other candidate materials. The 40-cm AlF_3-^{60}Ni interlayer material was chosen as the moderator-2. In the case, $\phi_{epithermal}$ was 6.96×10^9 n cm^{-2} s^{-1}, $\phi_{epithermal}/\phi_{fast}$ value was 38.41, and $\dot{D}_{fast}/\phi_{epithermal}$ was 1.71×10^{-14} Gy cm^2. The three values met the requirements of corresponding limits. However, $\phi_{epithermal}/\phi_{thermal}$ value was 9.94, and $\dot{D}_{\gamma}/\phi_{epithermal}$ was 5.83×10^{-13} Gy cm^2. These two values did not meet the recommended limits. Therefore, thermal neutron and gamma filters are required to reduce the thermal neutron and gamma photon dose.

Thermal neutron and γ filters

Two thermal neutron filter candidate materials, metallic lithium and cadmium, were examined in this study (Fig. 11). With the stronger thermal neutron absorption performance and better epithermal neutron flux maintaining performance, cadmium with thickness of 0.1 cm was chosen as the thermal neutron filter. In this case, the $\phi_{epithermal}/\phi_{thermal}$ value was about 200. The major drawback of cadmium is the high energy gamma ray yield in neutron capture reaction, but this problem may be solved by the γ filter layer. γ rays can be attenuated with bismuth. Figure 12 shows the $\dot{D}_{\gamma}/\phi_{epithermal}$ ratio for bismuth as a function of its thickness. Bismuth with the thickness of 4 cm was chosen as γ filter and $\dot{D}_{\gamma}/\phi_{epithermal}$ ratio was reduced to 1.37×10^{-13} Gy cm^2, which was lower than the recommended limit, 2×10^{-13} Gy cm^2.

Reflector and collimator

In order to reduce the neutron leakage and to increase the output neutron flux, the lead reflector was designed to wrap the multiplier and moderator-1. An arch structure design was adopted at the interface between the moderator-1 and

Table 6 BNCT in-air parameters of our proposed BSA and previous studies

Configuration	Yield ($\times 10^{14}$ n s^{-1})	$\phi_{epithermal}$ ($\times 10^{9}$ n cm^{-2} s^{-1})	$\phi_{epithermal}/\phi_{fast}$	$\phi_{epithermal}/\phi_{thermal}$	$\dot{D}_{fast}/\phi_{epithermal}$ ($\times 10^{-13}$ Gy cm^2)	$\dot{D}_{\gamma}/\phi_{epithermal}$ ($\times 10^{-13}$ Gy cm^2)	J/ϕ
Limits		>1	>20	>100	<2	<2	~0.7
Proposed facility	1.0	4.18	25.72	169.21	0.49	1.38	0.67
Rasouli et al. [13]	1.45	4.43	23.75	121.20	0.59	1.98	0.61
Cerullo et al. [28]	1.0	0.66	23.2	133	3.19	1.1	0.58
Cerullo et al. [29]	4.0	2.51	14.4	1114.5	3.45	0.21	0.57
Rasouli and Masoudi [21]	0.05	1.04	–	20.21	0.67	5.79	0.60

the reflector to improve the neutron beam performance at the beam port (Table 5). The arch reflector and the vertical reflector refer to the shape of the interface between the moderator-1 and the reflector. As shown in the Table 5, the neutron flux and $\phi_{epithermal}/\phi_{fast}$ value are improved by the arch reflector.

The lead collimator around the moderator-2 and filters was also designed to focus the neutron beam within the area with the diameter of 12 cm. In addition, in order to reduce the particle leakage along the direction of the neutron beam output, lithiated polyethylene (poly-Li) with the thickness of 7 cm was used as the neutron shield to effectively improve the performance of the neutron beam profile. According to the simulation results, epithermal neutron flux at 12 cm from the central axis was reduced to one-seventh of the epithermal neutron flux at the central axis.

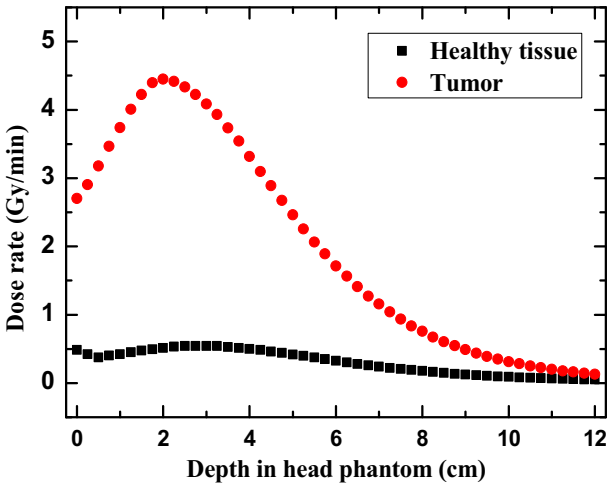

Fig. 15 Comparison of depth dose profiles between tumor and normal tissue

The in-air parameters of our BSA

Each part of the BSA was optimized to obtain the optimum BSA based on the D-T neutron generator. Based on the above design, the detailed dimensions and materials of the suggested BSA are shown in Fig. 13. The deuteron beam bombarded the tritium target and generated neutrons at the center of the multiplier. The arrow labeled "*d*" represented the deuteron beam in the neutron generator.

The neutron spectra at the beam port of the final BSA configuration is shown in Fig. 14. The output neutron beam has satisfied our desired epithermal neutron energy. The BNCT in-air parameters of our proposed BSA and previous studies are shown in Table 6. Based on the D-T neutron generator with the yield of 1×10^{14} n s^{-1}, our proposed BSA provided relatively high epithermal neutron flux which could reduce the irradiation times. Due to the reasonable structure design and material selection, $\phi_{epithermal}/\phi_{fast}$ was improved while maintaining the high

Table 7 In-phantom parameters of the proposed designed BSA and previous studies

Facility	ADDR (cGy min^{-1})	TT (min)	AD (cm)	TD (cm)	AR
Proposed facility	54.4	23	9	7.25	6.3
Torabi et al. [30]	70	17.8	7.6	5.8	4.2
THOR [31]	50	25	8.9	5.6	–
FiR1 [31]	45	30	9	5.8	–
R2-0 [31]	67	20	9.7	5.6	–
Rasouli et al. [13]	41.3	30.2	9.4	7	–
Rasouli and Masoudi [21]	50.35	24.8	8	5.89	4.26
Kononov et al. [32]	100	12.5	9.1	–	–

epithermal neutron flux, which was higher than other designs. Compared with the previously published studies, the impurity components of our proposed neutron beam were relatively low and the beam directionality was reasonable. Therefore, our neutron beam made a good balance between high neutron flux and high beam quality.

The in-phantom parameters of our BSA

In the dosimetric assessment study, neutron and γ fluxes were converted into dose values with kerma factors [26]. The dose was calculated as a function of the depth of the head phantom in the beam direction. The depth dose profile between tumor and normal tissue was plotted (Fig. 15). The In-phantom parameters of the proposed designed BSA and some other facilities are presented in Table 7. The ADDR value is about 54.4 cGy min^{-1} at the depth of 2.5 cm inside the phantom. The maximum allowable dose for the healthy tissue is 12.5 Gy and TT value can be estimated about 23 min, which is fairly feasible. The AD value of the neutron beam is 9 cm; the TD value is 7.25; the AR value is 6.3. After the treatment, the maximum dose in the skin tissue is 11.1 Gy and the 30 RBE-Gy tumor depth is 6.75 cm. Therefore, it can meet the requirements of the deep-seated brain tumor treatment.

Conclusions

The BNCT facilities based on the D-T neutron generator are compact and convenient deployment in hospitals. The optimization design of BSA based on a D-T neutron generator is relatively difficult due to the high initial energy of the neutrons. Better structure design and material combination are critical to improve the intensity and quality of the epithermal neutron beam. In this study, a BSA for BNCT was designed based on the neutron generator device with the neutron yield of 1×10^{14} n s^{-1}. The epithermal neutron flux of our model at the beam port was 4.18×10^9 n cm^{-2} s^{-1} due to the reasonable structure design and material selection. In BSA optimization, a comprehensive discussion on moderator optimization was conducted. With D_2O-^{54}Fe and AlF_3-^{60}Ni interlayer materials as moderator, the $\phi_{epithermal}/\phi_{fast}$ value was increased to 25.72 while maintaining the high epithermal neutron flux. The parameters of our proposed BSA met the limits of the in-air parameters. In the dosimetric assessment, the Therapeutic Depth of our neutron beam reached 7.25 cm, and the Advantage Ratio was 6.3, which was relatively high. Therefore, our proposed neutron beam can meet the requirements of deep-seated brain tumor treatment.

Acknowledgments This work was supported by the National Natural Science Foundation of China (Grant No. 11475087), the National Science and Technology Support Program (Grant No. 2015BAI34H00), and the Priority Academic Program Development of Jiangsu Higher Education Institutions.

References

1. Haapaniemi A, Kankaanranta L, Saat R, Koivunoro H, Saarilahti K, Makitie A, Atula T, Joensuu H (2015) Boron neutron capture therapy in the treatment of recurrent laryngeal cancer. Int J Radiat Oncol Biol Phys 95:404–410
2. Wang LW, Chen YW, Ho CY, Liu YWH, Chou FI, Liu YH, Liu HM, Peir JJ, Jiang SH, Chang CW, Liu CS, Lin KH, Wang SJ, Chu PY, Lo WL, Kao SY, Yen SH (2016) Fractionated boron neutron capture therapy in locally recurrent head and neck cancer: a prospective phase I/II trial. Int J Radiat Oncol Biol Phys 95:396–403
3. Watanabe T, Tanaka H, Fukutani S, Suzuki M, Hiraoka M, Ono K (2016) L-Phenylalanine preloading reduces the $^{10}B(n, \alpha)^7Li$ dose to the normal brain by inhibiting the uptake of boronophenylalanine in boron neutron capture therapy for brain tumours. Cancer Lett 370:27–32
4. Herrera MS, Gonzalez SJ, Burlon AA, Minsky DM, Kreiner AJ (2011) Treatment planning capability assessment of a beam shaping assembly for accelerator-based BNCT. Appl Radiat Isot 69:1870–1873
5. Harling OK, Riley KJ (2003) Fission reactor neutron sources for neutron capture therapy—a critical review. J Neurooncol 62:7–17
6. Kasesaz Y, Khalafi H, Rahmani F (2014) Design of an epithermal neutron beam for BNCT in thermal column of Tehran research reactor. Ann Nucl Energy 68:234–238
7. MoussaouiF EI, Bardouni T EI, Azahra M, Kamili A, Boukhal H (2008) Monte Carlo calculation for the development of a BNCT neutron source (1 eV–10 KeV) using MCNP code. Cancer/Radiothérapie 12:360–364
8. Elshahat BA, Naqvi AA, Maalej N, Abdalla K (2007) Design calculations of an accelerator based BSA for BNCT of brain cancer. J Radioanal Nucl Chem 274:539–544
9. Imoto M, Tanaka H, Fujita K, Mitsumoto T, Ono K, Maruhashi A, Sakurai Y (2011) Evaluation for activities of component of cyclotron-based epithermal neutron source (C-BENS) and the surface of concrete wall in irradiation room. Appl Radiat Isot 69:1646–1648
10. Capoulat ME, Herrer MS, Minsky DM, Gonzalez SJ, Kreiner AJ (2014) 9Be(d, n) 10B-based neutron sources for BNCT. Appl Radiat Isot 88:190–194
11. Lou TP (2003) Compact D-D/D-T neutron generators and their applications. Ph.D Thesis, University of California, Berkeley
12. Martin G, Abrahantes A (2004) A conceptual design of a beam-shaping assembly for boron neutron capture therapy based on deuterium–tritium neutron generators. Med Phys 31:1116–1122
13. Rasouli FS, Masoudi SF, Kasesaz Y (2012) Design of a model for BSA to meet free beam parameters for BNCT based on multiplier system for D-T neutron source. Ann Nucl Energy 39:18–25
14. Faghihi F, Khalili S (2013) Beam shaping assembly of a D-T neutron source for BNCT and its dosimetry simulation in deeply-seated tumor dosimetry simulation in deeply-seated tumor. Radiat Phys Chem 89:1–13
15. Yanch JC, Zhou XL, Brownell GL (1991) Monte Carlo investigation of the dosimetric properties of monoenergetic neutron beams for neutron capture therapy. Radiat Res 126:1–20
16. Koivunoro H, Bleuel DL, Nastasi U, Lou TP, Reijonen J, Leung KN (2004) BNCT dose distribution in liver with epithermal D-D and D-T fusion-based neutron beams. Appl Radiat Isot 61:853–859

17. Liskien Horst, Paulsen Arno (1973) Neutron production cross section and energies for the reactions T(p, n)3He, D(d, n)3He, and T(d, n)4He. Nucl Data Tables 11:569–619
18. Uhlar R, Kadulova M, Alexa P, Pistora J (2014) A new reflector structure for facility thermalizing D-T neutrons. J Radioanal Nucl Chem 300:809–818
19. Verbeke JM, Vujic JL, Leung KN (2000) Neutron beam optimization for boron neutron capture therapy using the D-D and D-T high-energy neutron sources. Nucl Technol 129:257–278
20. Eskandari MR, Kashian S (2009) Design of moderator and multiplier systems for D-T neutron source in BNCT. Ann Nucl Energy 36:1100–1102
21. Rasouli FS, Masoudi SF (2012) Design and optimization of a beam shaping assembly for BNCT based on D-T neutron generator and dose evaluation using a simulated head phantom. Appl Radiat Isot 70:2755–2762
22. Verbeke JM, Costes SV, Bleuel D, Vujic J, Leung KN (1998) Designing an epithermal neutron beam for boron neutron capture therapy for the fusion reactions $^{2}H(d,n)^{3}He$ and $^{3}H(d,n)^{4}He$, Lawrence Berkeley National Laboratory
23. Kiger WS, Sakamoto S, Harling OK (1999) Neutronic design of a fission converter-based epithermal neutron beam for neutron capture therapy. Nucl Sci Eng 131:1–22
24. Snyder WS, Ford MR, Warner GG, Fisher HR Jr (1969) Estimates for absorbed fractions for mono-energetic photon sources uniformly distributed in various organs of a heterogeneous phantom. J Nucl Med 3:47
25. ICRU Report46 (1992) Photon, electron, proton, and neutron interaction data for body tissues. International Commission on Radiation Units and Measurements, Bethesda
26. Albritton JR (2009) Computational aspects of treatment planning for neutron capture therapy, MIT Ph.D Thesis, Department of Nuclear Engineering
27. IAEA-TECDOC-1223 (2001) Current status of neutron capture therapy. International Atomic Energy Agency. IAEA, Vienna
28. Cerullo N, Esposito J, Leung KN, Custodero S (2002) An irradiation facility for boron neutron capture therapy application based on a radio frequency driven D-T neutron source and a new beam shaping assembly. Rev Sci Instrum 73:3614–3618
29. Cerullo N, Esposito J, Daquino GG (2004) Spectrum shaping assessment of accelerator-based fusion neutron sources to be used in BNCT treatment. Nucl Instrum Methods Phys Res Sect B. 213:641–645
30. Torabi F, Masoudi SF, Rahmani F, Rasouli FS (2014) BSA optimization and dosimetric assessment for an electron linac based BNCT of deep-seated brain tumors. J Radioanal Nucl Chem 300:1167–1174
31. Liu YWH, Huang TT, Jiang SH, Liu HM (2004) Renovation of epithermal neutron beam for BNCT at THOR. Appl Radiat Isot 61:1039–1043
32. Kononov OE, Kononov VN, Bokhovko MV, Korobeynikov VV, Soloviev A, Sysoev AS, Gulidov IA, Chub WT, Nigg DW (2004) Optimization of an accelerator-based epithermal neutron source for neutron capture therapy. Appl Radiat Isot 61:1009–1013